

C.P. HAURI<sup>1,✉</sup>  
J. GAUTIER<sup>2</sup>  
A. TRISORIO<sup>2</sup>  
E. PAPALAZAROU<sup>2</sup>  
P. ZEITOUN<sup>2</sup>

## Two-dimensional organization of a large number of stationary optical filaments by adaptive wave front control

<sup>1</sup> Paul Scherrer Institute (PSI), Villigen, Switzerland

<sup>2</sup> Laboratoire d'Optique Appliquée, ENSTA – Ecole Polytechnique, CNRS UMR 7639, 91761 Palaiseau, France

Received: 5 October 2007 / Revised version: 6 December 2007  
Published online: 19 January 2008 • © Springer-Verlag 2008

**ABSTRACT** We present an adaptive technique for the formation of multiple co-propagating and stationary filaments in a gaseous medium. Wavefront shaping of the initial beam is performed using a deformable mirror to achieve a complete two-dimensional control of the multi-spot intensity pattern in the laser focus. The spatial organization of these intensity spots yields reliable formation of up to five stable and stationary filaments providing a test bed for fundamental studies on multiple filamentation.

**PACS** 42.65.Jx; 52.38.Hb; 42.65.Sf

Beam break-up of a powerful laser into several filaments in space happens when the peak power of the laser pulse exceeds many times the critical power for self-focusing. The mechanism of multiple filament (MF) formation during self-focusing of a powerful laser was explained by transverse modulation instability (MI) in the spatial intensity profile giving rise to a splitting of the initial beam into small-scale cells, which trigger the formation of MF [1–3]. This mechanism is accompanied by stochastic shot-to-shot fluctuations of the initial laser beam [4], which may result in an arbitrary and non-stationary MF pattern being different for consecutive laser shots. Experimentally, different schemes have been successfully introduced to control MF formation. Deterministic MF patterns have been produced by imposing astigmatism on the laser beam with the help of a tilted lens [5], by use of anamorphic prisms to transform a Gaussian-like into an elliptical intensity beam profile [6] or by applying circularly polarized laser light [7]. Control of MF by those schemes, however, was restricted to one-dimensional transverse to the beam propagation. Experimental approaches towards a two-dimensional control of MF formation have recently been explored by use of a periodic mesh placed in the beam path for spatial regularization of a high-power femtosecond laser pulse [8] or by shaping the laser beam profile with spatial masks [9]. These techniques, however, suffer from substantial energy

losses and do not allow adaptive control of MF formation in space.

In this letter we use a reflective deformable mirror as an adaptive spatial phase shaper in order to gain a complete two-dimensional spatial control of the formation of a large number of stationary, independently co-propagating multiple filaments. We believe that our novel approach for organizing MF offers some noteworthy advantages over the techniques formerly described. First, no laser energy is sacrificed for our technique to work, since our scheme contains all-reflective optics and abstains lossy spatial masks. Second, contrary to a liquid-crystal-based wave front shaping technique recently used for stabilizing [10] and enhancing the beam quality of one single filament [11], the scheme presented here is scalable to the multi-TW level since deformable mirrors withstanding high flux are commercially available and routinely used in high power laser chains [12]. We believe that our approach is therefore of particular interest for laser-based atmospheric analysis techniques, such as femtosecond lidar, where the control of MF is crucial [13, 14] and where the optical element for controlling MF needs to sustain a high laser peak power ( $> 5$  TW). Third, our scheme is independent of the initial laser beam parameters, due to the adaptive nature of the deformable mirror, and offers a full two-dimensional control of the MF arrangement in space. Furthermore, the reliable and stable formation of MF provided by our scheme offers a test bed to study fundamental aspects of MF and to explore recent theoretical predictions of attraction, fusion, repulsion and spiral propagation of MF [15, 16]. Finally, many applications profit from controllable and stationary MF, such as filament-based ultrafast optical switches [17], multi-beam few-cycle femtosecond sources, and studies on propagation of MF in turbulent air [18].

Unlike the natural formation of MF, which has its origin in the MI triggered by the nonlinear response of the gas, our technique is based on active control of the laser energy distribution in the focal plane. This is achieved by wavefront shaping of the laser beam prior to the last focusing optics and linear propagation of the beam towards the geometrical focus where nonlinear pulse propagation (filamentation) sets in for individual focal spots due to an increase in peak intensities ( $> 10^{13}$  W/cm<sup>2</sup>). The formation of

✉ Fax: +41 56 310 4197, E-mail: christoph.hauri@psi.ch

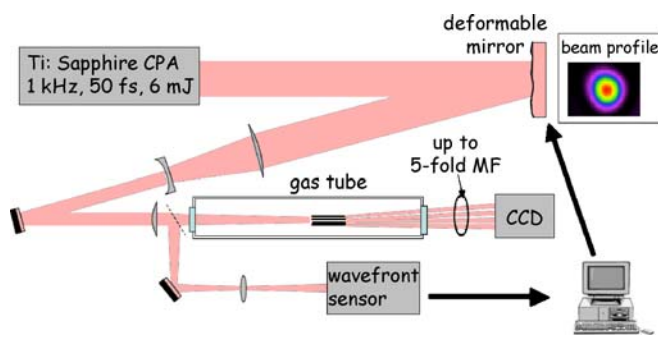


**FIGURE 1** Experimental setup for organizing multiple filaments by wavefront control. 1-kHz Ti:sapphire CPA system with deformable mirror (active area 1600 mm<sup>2</sup>, 31 actuators) steered by a computer; xenon-filled tube hosting multiple filaments; diagnostic tools like a CCD camera and a Shack–Hartmann wave front analyzer. The *inset* shows the intensity profile of the laser beam at the position of the deformable mirror

multiple intensity spots in the focus and consequently the formation of MF becomes controllable. Depending on the wavefront imposed by the laser beam the resulting intensity profile in the laser focus exhibits a specific number of transversely separated multiple foci. These foci are of different origin than the “hot-spots” stemming from MI since the multiple-focus pattern is existent even if the nonlinearity provided by the gas is not present (i.e., gas cell evacuated). Ideally, each of the multiple foci generated by wave front shaping only conveys a power high enough for driving filamentation, which results in the formation of a set of individual and stationary co-propagating filaments. Since a deformable mirror wavefront shaper provides control on the amount of power deposited in each individual intensity spot secondary filament splitting is avoided. Therefore, a stationary MF pattern is formed until the individual filament processes are terminated by both energy loss due to ionization and natural beam divergence.

For our proof-of-principle experiment, we used the 1-kHz high-power laser facility at LOA delivering linearly polarized 6-mJ, 40-fs pulses ( $\approx 0.15$  TW) with a Gaussian-like spatial beam profile. A deformable mirror of 45 mm in diameter equipped with 31 piezo-electric actuators (BIM31, Silas) is applied to manipulate the laser beam wave front, which is characterized by means of a commercially available Shack–Hartmann (SH) sensor (HASO, Imagine Optic). The SH sensor consists of a set of lenslets arranged in a matrix of  $32 \times 40$  and is placed in the plane conjugated to the deformable mirror to provide optimal conditions for wave front optimization. Due to the radial symmetric beam profile the wave front is accurately reconstructed by a set of Zernike polynomials (ZP) up to order 33.

Reflected by the silver-coated deformable mirror the amplified laser beam is focused into a gas tube, after passing a telescope to match best conditions for filamentation (Fig. 1). The 3-m-long gas tube is filled with 1.5 bar xenon and sealed with fused silica windows (3 mm thick, 40 mm in diameter). Xenon has been chosen since it offers the lowest critical power ( $\approx 0.8$  GW at 1.5 bar) of all (non-radiating) rare gases. It is, therefore, mostly suited to provoke the largest number of MF. In principle, air or other gases could also be used, whenever the laser system provides enough peak power to launch MF.

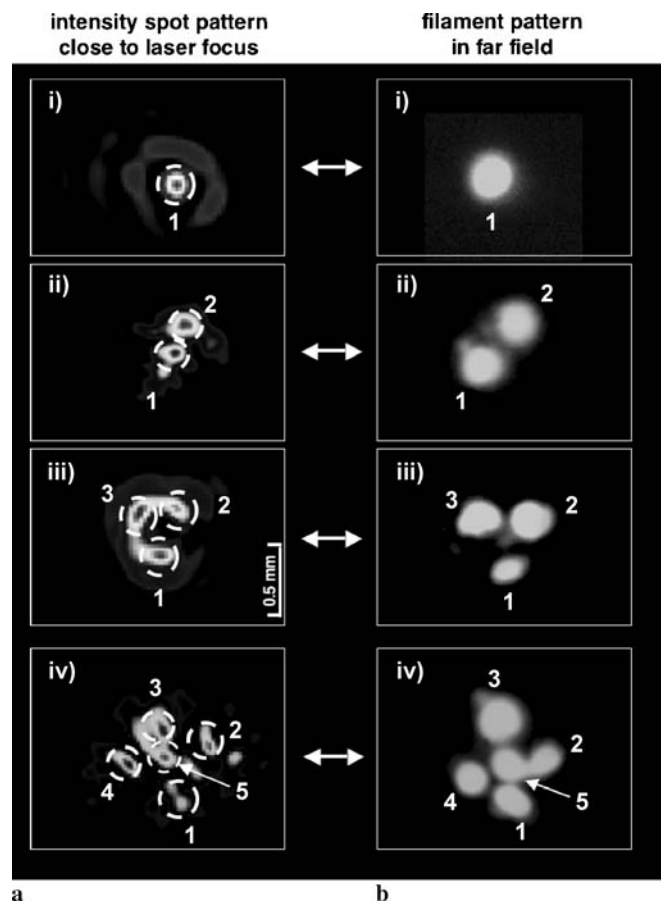


**FIGURE 2** (a) Beam intensity profiles in the proximity of the geometrical focus for different wave front configurations (see Fig. 2). Intensity spots with sufficient peak power for launching filamentation are marked by dashed circles for better visibility. (b) Pattern of stable multiple filamentation recorded by a CCD. The MF patterns (i)–(iv) are generated by corresponding intensity spot patterns depicted in (a). Each picture shows the integrated signal of 50 consecutive laser shots (integration time: 50 ms) indicating excellent stationary stability

Plotted in Fig. 2a are four different intensity distributions at a position a few millimeters in front of the geometrical focus where filamentation is supposed to set in. The intensity patterns are generated by imposing specific wave fronts (depicted in Fig. 3) on the amplified input pulse by means of the deformable mirror. The initial Gaussian-like beam profile as well as the input energy remained unchanged throughout the experiment. Initially, the laser wave front was optimized for best flatness ( $\text{rms} < 0.08\lambda$ ), yielding a very unstable MF pattern since  $P \gg P_{\text{crit}}$ . Our procedure for achieving the requested intensity pattern in the focal plane is based on online diagnostics of the laser focus and manual modification of the wave front by tailoring Zernike polynomial coefficients (see below). This procedure was successful for the formation of one (i), two (ii) three (iii) and more (iv) transversally separated spots in the focal plane as shown in Fig. 2a. The individual intensity spots exhibit all a diameter of 100–150  $\mu\text{m}$  and most of them (indicated by dashed white circles) carry sufficient energy for triggering self-focusing and filamentation.

Filamentation driven by the laser foci shown in Fig. 2a yields the MF pattern exposed in b. Depending on the number of intensity “hot-spots” one stationary filament (i) or multi-

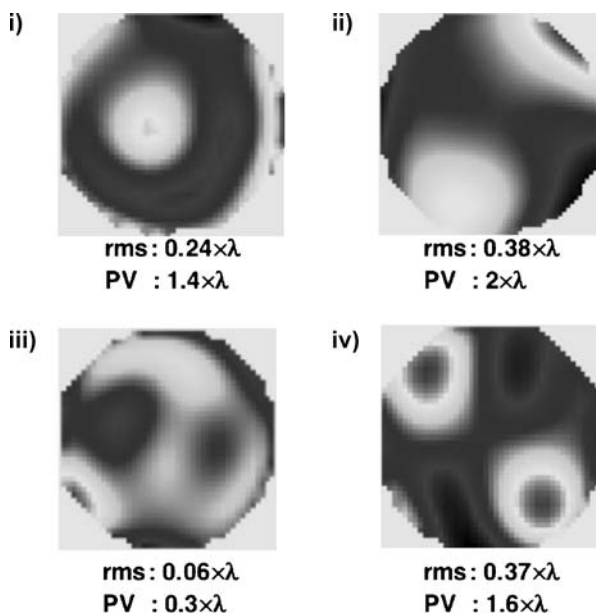


**FIGURE 3** Wave front shaping by a deformable mirror. The wave fronts (i)–(iv) are used to generate corresponding “hot-spot” intensity profiles (Fig. 1a,(i)–(iv)) in the geometrical focus. For each wave front the corresponding rms and peak-to-valley (PV) values are displayed

ple filaments with 2, 3 and 5 individual channels are observed (ii–iv). The laser intensity patterns in the focus (a) and the corresponding MF patterns recorded in the far field (b) are in very good agreement. Case (i), illustrating the formation of a single filament, is generated with the beam wave front shown in Fig. 2(i) deviating most of the energy outside the focal region into an annular profile. Three Zernike polynomial (ZP) coefficients have been modified, namely ZP 8 (third-order spherical aberration,  $0.14\lambda$ ), ZP 6 (coma  $0^\circ$ ,  $0.11\lambda$ ) and ZP 4 (astigmatism  $0^\circ$ ,  $0.09\lambda$ ). The remaining single intensity spot in the center of the beam with roughly  $550\mu\text{J}$  is powerful enough to drive non-linear propagation while the annular part keeps its linear propagation and does not undergo filamentation due to the low intensity.

A well-resolved twin configuration of intensity spots (a,(ii)) is generated by introducing astigmatism at  $0^\circ$  (ZP 5,  $0.24\lambda$ ) and  $45^\circ$  (ZP 6,  $0.1\lambda$ ) to the initially plane wave front resulting in a stationary formation of twin filaments (b,(ii)). The energies measured for filament 1 and 2 are  $490\mu\text{J}$  and  $500\mu\text{J}$ , respectively. Stable MF patterns with three independent self-guided channels are depicted in (b,(iii)) with the corresponding lateral focal spots arranged annularly around the beam propagation axis (a,(iii)). In this case three-foil at  $90^\circ$  (ZP 10) in combination with 5th-order astigmatism at  $0^\circ$  (ZP 11) are the major aberrations leading to the measured wave front shown in Fig. 3(iii). The energy carried by filament 1 (2, 3) is  $380\mu\text{J}$  ( $470\mu\text{J}$ ,  $490\mu\text{J}$ ) and its measurement is performed in the far-field (i.e., 5 m from the filament’s end) where the well-defined self-guided core (whitelight) can easily be separated from the reservoir (pure infrared radiation) by means of a diaphragm.

The MF patterns shown in (b) are recorded by a CCD camera three meters after the filaments’ end. To improve the quality of the pictures a color filter (BG39) was used to block the fundamental (i.e., non-filamenting) light of the amplifier and

the reservoir contribution. This filtering turned out to increase the image contrast especially for case (i)–(iii) (Fig. 2a) where most of the amplifier energy does not undergo filamentation and white-light generation but simply linear propagation. The strong IR background signal would therefore lead to a saturation of the CCD. The acquisition time for each picture was 50 ms, which corresponds to an integrated signal of 50 consecutive laser shots. The well-resolved and sharp patterns in Fig. 1b confirm that the role of noise in the organization of MF is tenuous in our experiment and that the spatial MF stability is excellent since no blurring is observed, even for a larger accumulation of shots ( $\approx 1000$ ). Note that for a perfectly (i.e., diffraction-limited) focused beam with a flat wave front, only stochastic filament patterns are observed resulting in a complete blurring of the pictures shown in Fig. 1b even for an accumulation of 50 consecutive laser shots.

In general, the largest possible number of stable filaments is restrained by the pulse energy of the amplifier and the capability of the beam wave front shaper to generate well-resolved hot spots in the focus. Our experimental conditions as well as our simple manual procedure for shaping the wave front allows the formation of maximal five independent filaments, as shown in Fig. 2b,(iv). This MF pattern demonstrates the beautiful arrangement of five individually propagating plasma waveguides launched by the corresponding intensity spots depicted in Fig. 2a,(iv). To achieve the complex energy distribution in the focus the plane laser wave front is distorted by astigmatism at  $0^\circ$  (ZP 5), 5th-order astigmatism at  $45^\circ$  (ZP 12) and tetrafoil at  $0^\circ$  (ZP 16). The energies transported in the individual filaments are measured to be  $450\mu\text{J}$  for filament 2 and  $480\text{--}500\mu\text{J}$  for filament 1, 3, 4 and 5, respectively. The intensity pattern in (iv) reveals that the formation of well-resolved multi-spots is challenging by manually adapting the wavefront since the optimal wave front is composed by a larger ( $> 3$ ) number of Zernike polynomials than required for MF pattern shown in case (i)–(iii). Not all of the visible intensity spots carry sufficient energy for self-focusing which prevents those beams from filamenting. Formation of more sophisticated intensity distributions in the focal plane requires therefore an iterative or adaptive learning algorithm to optimize a set of specific Zernike polynomials. We believe that such an optimization procedure is of particular interest when a more powerful laser is used for two-dimensional arrangement of a large number of filaments as requested by femtosecond lidar applications, for example.

In conclusion we have demonstrated an adaptive and complete two-dimensional control of multiple filamentation by wave front shaping of the amplified laser beam. The deformable mirror in combination with a Shack–Hartmann sensor is shown to be a powerful scheme to achieve stationary multi-filament patterns by introducing higher-order phase aberrations to the initial beam wave front. Such stable MF formation with up to five individual filaments can serve as a test bed to explore fundamental aspects of MF and is of interest for many applications including multi-beam few-cycle sources and ultrafast optical switches. The scalability of our scheme to the TW level offers the potential for well-resolved MF-based atmospheric remote sensing applications and for the study fundamental aspects of MF in (turbulent) air.

## REFERENCES

- 1 A. Campillo, S. Shapiro, B. Suydam, Appl. Phys. Lett. **23**, 628 (1973)
- 2 A. Campillo, S. Shapiro, B. Suydam, Appl. Phys. Lett. **24**, 178 (1974)
- 3 S. Skupin, L. Bergé, U. Peschel, F. Lederer, G. Mejean, J. Yu, J. Kasparian, E. Salmon, J.P. Wolf, M. Rodriguez, L. Woeste, R. Bourayou, R. Sauerbrey, Phys. Rev. E **70**, 46602 (2004)
- 4 V.I. Bespalov, V.I. Tantalov, J. Exp. Theor. Phys. Lett. **3**, 307 (1966)
- 5 G. Fibich, S. Eisenmann, B. Ilan, A. Zigler, Opt. Lett. **29**, 1772 (2004)
- 6 T.D. Grow, A.L. Gaeta, Opt. Express **13**, 4594 (2005)
- 7 A. Trisorio, C.P. Hauri, Opt. Lett. **32**, 1650 (2007)
- 8 V.P. Kandidov, N. Akozbek, M. Scalora, O.G. Kosareva, A.V. Nyakk, Q. Luo, S.A. Hosseini, S.L. Chin, Appl. Phys. B **80**, 267 (2005)
- 9 G. Mechain, A. Couairon, M. Franco, B. Prade, A. Mysyrowicz, Phys. Rev. Lett. **93**, 0350031 (2004)
- 10 T. Pfeiffer, L. Gallmann, M. Abel, D. Neumark, S. Leone, Opt. Lett. **31**, 2326 (2006)
- 11 D. Walter, S. Eyring, J. Lohbreier, R. Spitzenpfeil, C. Spielmann, Appl. Phys. B **88**, 175 (2007)
- 12 Y.K. Ma, J. Akahane, Y. Aoyama, M. Fukuda, Y. Kiriya, H. Tajima, T. Kudryashov, A. Sheldakova, *Wavefront Correction of a 100-TW, 10-Hz Ti:sapphire Laser System and the Method Aiming at  $10^{23}$  W/cm<sup>2</sup> in a Petawatt Ti:sapphire Amplifier Chain* (Laser and Electro-Optics Society, Sidney, 2005), p. 617
- 13 J. Kasparian, M. Rodriguez, G. Mejean, J. Yu, E. Salmon, H. Wille, R. Bourayou, S. Frey, Y.B. Andre, A. Mysyrowicz, R. Sauerbrey, J.P. Wolf, L. Woeste, Science **301**, 61 (2003)
- 14 L. Berge, S. Skupin, F. Lederer, G. Mejean, J. Yu, J. Kasparian, E. Salmon, J.P. Wolf, M. Rodriguez, L. Woeste, R. Bourayou, R. Sauerbrey, Phys. Rev. Lett. **92**, 225002 (2004)
- 15 S.A. Hosseini, Q. Luo, B. Ferland, W. Liu, S.L. Chin, O. Kosareva, N.A. Panov, N. Akozbek, V.P. Kandidov, Phys. Rev. A **70**, 033802 (2004)
- 16 T. Xi, X. Lu, J. Zhang, Phys. Rev. Lett. **96**, 025003 (2006)
- 17 J. Liu, H. Schroeder, S.L. Chin, R. Li, Z. Xu, Appl. Phys. Lett. **87**, 161105 (2005)
- 18 S.L. Chin, A. Talebpour, J. Yang, S. Petit, V.P. Kandidov, O.G. Kosareva, M.P. Tamarov, Appl. Phys. B **74**, 67 (2002)